Hydrodynamic characteristics of transient Ni-like x-ray lasers

Y. J. Li and J. Zhang*
Laboratory of Optical Physics, Institute of Physics, Chinese Academy of Science, Beijing 100080, People's Republic of China
(Received 7 August 2000; revised manuscript received 23 October 2000; published 27 February 2001)

A simple similarity model is presented to study the hydrodynamics of transient collisional excitation nickellike x-ray lasers. Scaling laws for the temperature, scale length, and electron density are obtained by analytic derivation. The hydrodynamic characteristics of transient Ni-like Pd x-ray lasers are investigated using this model. The calculations agree well with Dunn's experimental results.

DOI: 10.1103/PhysRevE.63.036410 PACS number(s): 52.59.Ye, 42.55.Vc

I. INTRODUCTION

Two main objectives on developing x-ray lasers are to deliver a coherent, monochromatic, saturated output at successively shorter wavelengths toward, the ''water window'' and to provide a ''table-top'' x-ray laser for applications [1–3]. ''Traditional'' collisionally pumped Ni-like x-ray lasers are believed to be more promising to provide the saturated output in the spectral band near the ''water window'' [4,5]. However, the efficiency of the ''traditional'' collisional excitation schemes is still far below the requirements for the ''table-top'' operation mode.

Recently, a novel transient collisional excitation (TCE) scheme has been demonstrated by Nickles *et al.* for the Ne-like Ti $3p$-$3s$ ($J=0\rightarrow1$) transition at 32.6 nm, where a high gain of 19 cm^{-1} is measured with only a few Joule pump energy [6,7]. More recent results have been reported by Dunn *et al.* [8], where a gain coefficient of 35 cm^{-1} and a gain-length product of 12.5 were measured on the $4d$-$4p$ ($J=0\rightarrow1$) transition for the Ni-like Pd laser at 14.7 nm using only 5 J pump energy. This new scheme greatly enhances the efficiency of collisional excitation schemes by increasing the gain coefficient and shows us a way towards ''table-top'' x-ray lasers [9].

To date, the design and analysis of TCE x-ray lasers relies heavily on complicated one- or two-dimensional numerical simulations of hydrodynamics and atomic kinetics [10]. In this paper, we present a simple model for the TCE Ni-like x-ray lasers and make a detailed analysis using a set of self-similar, coupled ordinary differential equations. The purpose of our work is to understand the hydrodynamic characteristic of the transient collisional x-ray lasers and to provide a simple tool for experimentalists to quickly scan and optimize parameters to design experiments.

II. SIMILARITY EQUATIONS AND EQUATION OF STATE

The ''standard'' TCE x-ray lasers are pumped [8] by a combination of irradiation of nanosecond and picosecond laser pulses. The nanosecond laser pulse is used to create an optimized preplasma with Ni-like (or Ne-like) ionization stage and longer scale length. Then, the picosecond pulse heats plasma rapidly to reach required conditions with high electron temperature while keeping a low ion temperature. This is beneficial to produce high gain because the gain coefficient is proportional to the electron temperature and inversely proportional to the square root of the ion temperature.

It is well known that the region of interest for x-ray laser gain is the corona region of $n_e<n_c$ and there is an isothermal expansion region during the pulse. The velocity distributions of electrons and ions reach their own Maxwellian equilibrium in this region, respectively. Because the mass of the ions is much heavier than that of the electrons, we assume that the ions are a background of the electrons and plasma is an ideal gas. Thus single-fluid, ideal hydrodynamic equations are adopted in the work,

$$\frac{\partial\rho}{\partial t}+\frac{\partial\rho v}{\partial x}=0, \tag{1}$$

$$\rho\left(\frac{\partial v}{\partial t}+v\frac{\partial v}{\partial x}\right)=-\frac{\partial p}{\partial x}, \tag{2}$$

$$\frac{\partial}{\partial t}\left[\rho\left(\varepsilon+\frac{v^2}{2}\right)\right]=-\frac{\partial}{\partial x}\left[\rho v\left(\varepsilon+\frac{v^2}{2}\right)+\rho v\right]+\rho H, \tag{3}$$

where x is the spatial coordinate measured perpendicular to the slab surface; t is time; ρ, v, p, and T are the mass density, velocity, pressure, and temperature, respectively; ε is the internal energy per unit mass; and H is the net heating rate per unit mass. The equation of state and the laser heat deposition will be discussed below.

To obtain the similarity equations, we assume that the expansion of the plasma is homogeneous and satisfies the rarefactional wave solution varied with time:

$$v=C_s+x/t, \tag{4}$$

where C_s is the transient isothermal sound speed ($C_s=\sqrt{TZ/M_i}=T^{1/2}Z^{1/2}/M_i^{1/2}$). The momentum equation [Eq. (2)] separates in space and time with these assumptions. The solution of the spatial part (at constant time) gives an exponential attenuation density profile, which is normalized with the continuity equation,

$$\rho=m/L\,\exp(-x/L), \tag{5}$$

*Author to whom correspondence should be addressed. Email address: Jzhang@aphy.iphy.ac.cn

where m is the mass ablated by the laser pulse from the slab target and L is the scale length of the plasma. With the equation of the mass ablation rate derived by De Groot *et al.* [11], which is valid for the ablation process of the thick slab target irradiated by a ns laser pulse, we derive the relations between the ablation mass and the intensity of the drive laser and the target element with the assumption of a homogeneous process of the ablation:

$$m = m_0 t^{2/3}, \tag{6}$$

where

$$m_0 = 2.55\times 10^{-13} I^{2/3}[A/(Z+1)]^{7/6}/(Z\ln\Lambda)^{1/3}, \tag{7}$$

where the unit of m is g/cm^2, the unit of t is ns, the unit of I is W/cm^2, A is the atomic number of the element, Z is the average charge of ion, and $\ln\Lambda$ is the natural Coulomb logarithm. With the assumption of the homogeneous expansion, the momentum and energy equations can be simplified to

$$LC_s\left(\frac{l}{2}\frac{d\ln T}{dt}+1\right)=\frac{pt}{\rho}, \tag{8}$$

$$C_v\frac{dT}{dt}=H-\frac{p}{\rho t}, \tag{9}$$

where C_v ($\equiv d\varepsilon/dT$) is the specific heat per unit mass.

The laser heating rate changes with $\tau_{\rm ib}$, i.e., $H \approx I\tau_{\rm ib}/m$, when $\tau_{\rm ib}<1$, while the laser heating rate is a constant, i.e., $H\approx I/m$, when $\tau_{\rm ib}>1$, where $\tau_{\rm ib}$ is the inverse bremsstrahlung optical depth through the plasma:

$$\tau_{\rm ib}=\int \kappa_{\rm ib}dx. \tag{10}$$

The opacity $\kappa_{\rm ib}$ is determined by the following equation [12]:

$$\kappa_{\rm ib}=\left(\frac{2}{\pi}\right)^{1/2}\frac{4}{3}\left(\frac{Zn_e^2e^6\lambda^2\ln\Lambda}{c^3(m_cT)^{3/2}(1-n_c^2/n_c^2)^{1/2}}\right), \tag{11}$$

where λ is the laser wavelength, n_e is the electron density, n_c is the critical density ($\approx 1.1\times 10^{21}/\lambda^2\ {\rm cm}^{-3}$), T is the electron temperature in energy unit, m_e is the electron mass, and c is the light velocity.

In the corona region of $n_e \leqslant n_c$, electron temperature is higher than a few tens eV, and the corona model for the average charge of ion may be adopted [13]:

$$Z\approx \tfrac{2}{3}[AT_e(eV)]^{1/3}. \tag{12}$$

The formulas we use for the EOS are

$$p=ZT\rho/M, \quad \text{and} \quad C_v=\tfrac{3}{2}Z/M_i \tag{13}$$

where M_i is the ion mass.

TABLE I. Normalized values for scaled variables.

Physical variable	Symbol	Normalized value
Time	t	1 ns
Laser intensity	I	10^{14} W m^{-2}
Laser wavelength	λ	1.053 μm
Ablation mass	m	10^{-4} g cm^{-2}
Ion charge	Z	65
Atomic mass	A	240
Coulomb logarithm	Λ	5

III. ANALYTIC SOLUTIONS OF THE SIMILARITY EQUATIONS

Useful scaling laws for plasma variables have been derived from analytic solutions for flat-top laser pulses by using a similarity model of the Ni-like scheme. We employed convenient units listed in Table I [14] and scaled the variable with underlines in the whole derivation in order to simplify the calculation. Two distinct periods for the long pulse ($0 < t \leqslant t_{1L}$ and $t_{1L} \leqslant t \leqslant t_m$, where $\underline{t}_{1L}=\Delta\underline{t}_{1L}$ is the long pulse duration and t_m is the delay between the long pulse and the short pulse) and two distinct periods for the short pulse ($t_m \leqslant t \leqslant t_{2L}$ and $t \geqslant t_{2L}$, where $\underline{t}_{2L}=t_m+\Delta\underline{t}_{2L}$ and $\Delta\underline{t}_{2L}$ is the short pulse duration) are adopted in order to clearly show the physics process in the calculation.

A. Analytic solutions for the long laser pulse

The purpose for the long laser pulse is to produce a long scale length plasma with optimized initial conditions; the heating and ionization processes take place for the whole pulse duration. The laser energy is mainly deposited near the critical density.

1. During the time of $t \leqslant t_{1L}$

During the time of $t \leqslant t_{1L}$, an expression for the optical depth is obtained by integrating Eq. (10) over the density profile since the heating and ionization processes take place in the region where the electron density is close to the critical density [13]. That is,

$$\tau_{\rm ib}=5.757\sqrt{\pi}\times 10^{-3}\underline{m}^2\underline{A}^2\underline{Z}^3\underline{\Lambda}\underline{\lambda}^2T^{3/2}\underline{L}, \tag{14}$$

where $\underline{\Lambda}$ is taken as a constant in the corona. Solving Eqs. (8) and (9) with Eqs. (6), (12), and (13), the analytic solutions satisfying the similarity equations, after the influence of the initial conditions disappeared, i.e., taking $\tau_{\rm ib}<1$, are

$$T=3.902\ {\rm keV}\underline{I}^{5/9}\underline{A}^{2/9}\underline{\Lambda}^{2/9}\underline{\lambda}^{2/3}\underline{t}^{2/9}. \tag{15a}$$

Because t is close to t_{1L}, the temperature is kept nearly constant due to a balance of laser heating with expansion cooling, see Fig. 1,

$$L=2.87\times 10^{-2}\ {\rm cm}\ \underline{I}^{10/27}\underline{A}^{-2/27}\underline{\lambda}^{4/9}\underline{\Lambda}^{4/27}\underline{t}^{31/27}, \tag{15b}$$

$$n_0=20.82\times 10^{20}\ {\rm cm}^{-3}\underline{I}^{11/54}\underline{A}^{4/27}\underline{\lambda}^{-5/9}\underline{\Lambda}^{-2/54}\underline{t}^{-14/27}, \tag{15c}$$

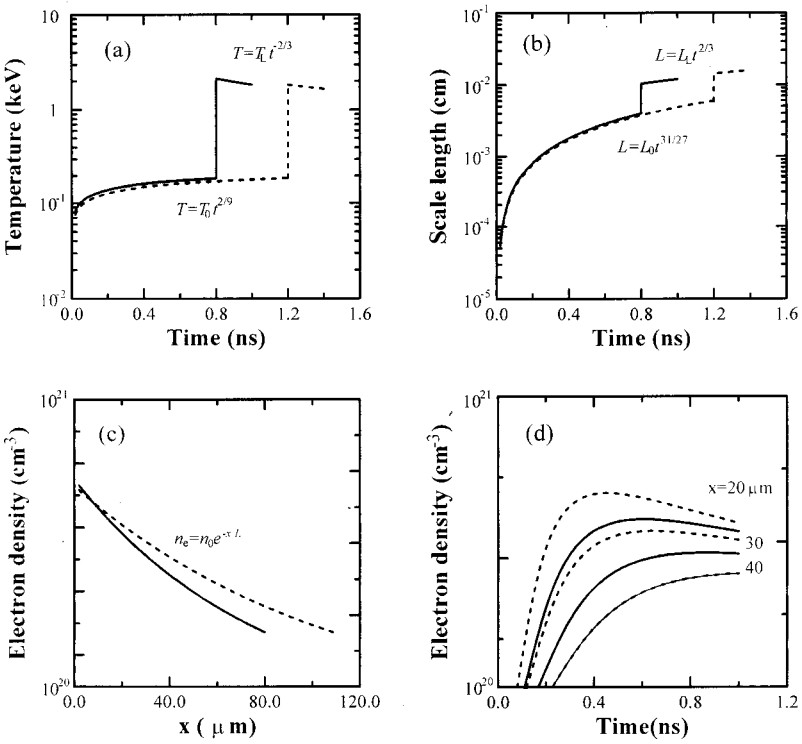

FIG. 1. (a) Temporal history for electron temperature, (b) scale length history, (c) electron density vs x at the center of the pulse, and (d) electron density history at different x for different long pulse duration of a flat-top pulse with the same short pulse conditions. The solid line is the solutions for $I_1=0.7\times10^{12}$ W/cm^2, $\lambda=1.053$ μm, $\Delta t_{IL}=0.8$ ns, $I_2=5.2\times10^{14}$ W/cm^2, and $\Delta t_{2L}=1.1$ ps. The dashed line is the solutions for $I_1=0.6\times10^{12}$ W/cm^2, $\lambda=1.053$ μm, $\Delta t_{IL}=1.2$ ns, $I_2=5.2\times10^{14}$ W/cm^2, and $\Delta t_{2L}=1.1$ ps.

where n_0 is the maximum value of n_e. Using Eq. (5), we can determine the electron density for position x and time t with Eq. (15c).

2. During the time of $t_{1L}\leqslant t\leqslant t_m$

After the time t_{1L}, the long laser pulse is turned off and the plasma continues to expand adiabatically. The exact analytical solutions can be obtained for this period using the condition before t_{1L}:

$$T=T_{1L}\underline{t}_{1L}^{2/3}\underline{t}^{-2/3}, \tag{16a}$$

$$L=L_{1L}\underline{t}_{1L}^{-5/9}\underline{t}^{5/9}, \tag{16b}$$

$$n_o=n_{1L}\underline{t}_{1L}^{7/9}\underline{t}^{-7/9}, \tag{16c}$$

where T_{1L}, L_{1L}, and n_{1L} are the electron temperature, scale length, and electron density at t_{1L}.

B. Analytic solutions for the short laser pulse

For the case of a ''standard'' transient collisional x-ray laser, the second pulse is so short that we can believe the following. First, we can assume that $m=m_0t_{1L}^{2/3}$ is a constant after the time t_{1L} and the heating rate is constant after the time t_m $(H=I/m)$ with $\tau_{\rm ib}>1$ because the preplasma is not transparent for the second pulse since the transparent temperature is proportional to the three-fourth power of the intensity. Second, there is not enough time to *change the state of ion charge*. This means Z can be taken as a constant. The formula we use for the EOS here is Eq. (13).

1. During the time of $t_m\leqslant t\leqslant t_{2L}$

At time t_m, when the second short laser pulse has started, the solutions can be obtained by considering the initial conditions before t_m:

$$T=23.123\,\text{keV}\,\underline{I}_2\underline{m}^{-1}\underline{A}\,\underline{Z}^{-1}\underline{t}\left(1-t_m^{5/3}t^{-5/3}+\frac{T_nt_m^{2/3}}{T_2}t^{-5/3}\right), \tag{17a}$$

where T_m is the electron temperature at t_m, $T_2=23.123\,\text{keV}\underline{I}_2\underline{m}^{-1}\underline{A}\underline{Z}^{-1}$,

$$L=5.164\times10^{-2}\,\text{cm}\,\underline{I}_2^{1/2}\underline{m}^{-1/2}\underline{t}^{3/2}\times\left(1-t_m^{5/3}t^{-5/3}+\frac{L_m^2}{L_2^2t_m^{4/3}}t^{-5/3}\right)^{1/2}, \tag{17b}$$

where L_m is the scale length at t_m, $L_2=5.164\times10^{-2}\,\text{cm}\underline{I}_2^{1/2}\underline{m}^{-1/2}$,

$$n_0=3.157\times10^{20}\,\text{cm}^{-3}\underline{I}_2^{-1/2}\underline{m}^{3/2}\underline{A}^{-1}\underline{Z}\underline{t}^{-3/2}\times\left(1-t_m^{-5/3}t^{-5/3}+\frac{n_2^2\tau_m^{1/6}}{n_m^2}t^{-5/3}\right)^{-1/2}, \tag{17c}$$

where $\underline{n}_m$ is the electron density at t_m, $n_2=3.157\times10^{20}\,\text{cm}^{-3}\underline{I}_2^{-1/2}\underline{m}^{3/2}\underline{A}^{-1}\underline{Z}$.

2. During the time of $t_{2L}\leqslant t$

After the time t_{2L}, the second short laser pulse is turned off and the plasma continues to expand adiabatically. The analytical solutions can be obtained for this period using the condition before t_{2L}:

$$T = 23.123\,\mathrm{keV}\,\underline{I}_2\underline{m}^{-1}\underline{A}\,\underline{Z}^{-1}\underline{t}_{2L}^{5/3}\underline{t}^{-2/3} \times\left(1 - t_m^{5/3}t_{2L}^{-5/3} + \frac{T_m t_{nl}^{2/3}t_{2L}^{-5/3}}{T_2}\right), \tag{18a}$$

$$L = L_2 t_{2L}^{5/6}\underline{t}^{2/3}\left(1 - t_m^{5/3}t_{2L}^{-5/3} + \frac{L_m^2}{L_2^2}t_m^{2/3}t_{2L}^{-5/3}\right)^{1/2}, \tag{18b}$$

$$n_0 = n_2\underline{t}_{2L}^{-5/6}\underline{t}^{-2/3}\left(1 - t_m^{-5/3}t_{2L}^{-5/3} + \frac{n_2^2 t_{2L}^{-5/3}}{n_m^2\underline{t}_m^{2/3}}\right)^{-1/2}. \tag{18c}$$

IV. RESULTS AND DISCUSSION

It is well known that the laser energy is mainly deposited in the corona region of $n_e \leqslant n_c$. The model is more valid for heavy elements than for light elements [13]. This comes from the corona model of the average state of charge. In order to justify the model, we calculate the hydrodynamics of the transient collisional Ni-like Pd x-ray laser under the same experimental conditions as Ref. [8] and compare the results between our model calculation and the experiment.

The first goal for the long laser pulse is to produce more Ni-like ions. A longer constant temperature period is, of course, beneficial for the production of a sort of ions from Eq. (12). The electron temperature during the isothermal period is the two-ninth power of the time from Eq. (15a). This makes the temperature almost a constant at the later time during the long pulse. Thus, the longer the pulse duration is, the closer to a constant temperature for the later time the temperature is, as shown in Fig. 1(a). Simultaneously, the longer pulse duration can also make a longer scale length, as shown in Fig. 1(b). This is beneficial for the propagation of an x-ray laser pulse.

The second goal is to enhance efficiency. The law of enhancing efficiency is certainly to use the lower intensity to reach the electron temperature required by ionization for the long pulse. It will be highly efficient when the long pulse not only ionizes the plasma to the Ni-like ions, but also achieves thermodynamic equilibrium between electrons and ions. Thus, we define the ratio of time of the long pulse duration to the equilibrium time as a standard of approximation. The time of the thermodynamic equilibrium is

$$t_{ei} = \left(\frac{4\pi\varepsilon_0}{e^2}\right)^2 \frac{3m_i m_e^{-1/2}(T_e)^{3/2}}{8\sqrt{2\pi}Z^2 n_i(\log_{10}\Lambda)}. \tag{19}$$

Equation (19) can also be used to judge whether the short pulse duration is short enough to ignore the ionization change. We can neglect the change of Z if the ratio between the short pulse duration and the equilibrium time is smaller that 10^{-4}.

We calculated the Ni-like Pd ions for the long pulse under the same conditions of Dunn's experiment ($I_1 = 0.7 \times 10^{12}\,\mathrm{W/cm^2}$, $\lambda = 1.053\,\mu\mathrm{m}$, $t_{1L} = 0.8\,\mathrm{ns}$, slab target). The calculated results show that the maximum electron temperature during the long pulse is 188 eV, which can ionize the Pd to an average state of charge $Z = 18.1$, as shown by the solid line in Fig. 1(a). The scale length is about 40 μm, as the solid line shows in Fig. 1(b). The electron density is $7.52 \times 10^{20}\,\mathrm{cm^{-3}}$, as shown by the solid line in Fig. 1(c). However, the equilibrium time is about 1.4 ns. The t_{1L}/t_{ei} is about 0.57. For comparison, we also calculated the electron temperature and the average state of charge with the conditions of $I_1 = 0.6 \times 10^{12}\,\mathrm{W/cm^2}$, $\lambda = 1.053\,\mu\mathrm{m}$, $t_{1L} = 1.2\,\mathrm{ns}$, slab target and the same short pulse. The results are $T_e = 188.8\,\mathrm{eV}$, $Z = 18.1$, $L = 60\,\mu\mathrm{m}$, $n_e = 7.28 \times 10^{20}\,\mathrm{cm^{-3}}$, shown by the dashed line in Fig. 1. The equilibrium time is about 1.8 ns. The t_{1L}/t_{ei} is about 0.67. For the short laser pulse, the temperature is 1.84 keV under Dunn's condition and 2.07 keV in the second case. The equilibrium time is about 55.5 and 66.2 ns, respectively. The radio t_{2L}/t_{ei} is about 1.98×10^{-5} and 1.66×10^{-5}, respectively. It is clear that the pulse duration for the long pulses is shorter than the equilibrium time for both cases. However, it is more efficient for the second case than Dunn's case and the scale length is longer than Dunn's. The conclusion we get here is that the lower intensity and longer duration of the long laser pulse will be more beneficial to enhance the efficiency. The electron density history at different positions for the two cases is shown in Fig. 1(d).

In contrast with the period during the long pulse, the first important thing for the period during the short pulse is that T_e cannot be lower than ΔE_u [8], where ΔE_u is the upper laser level excitation energy. The reason for the requirement of $T_e > \Delta E_u$ is that we want to achieve the optimum gain. Here $\Delta E_u = 450.3\,\mathrm{eV}$. The calculation results show that the electron temperature during the short pulse is 1.84 keV under the same conditions of Dunn's experiment ($I_2 = 5.2 \times 10^{14}\,\mathrm{W/cm^2}$, $\lambda = 1.053\,\mu\mathrm{m}$, $t_{2L} = 1.1\,\mathrm{ps}$, slab target). This is about four times as large as $\Delta E_u = 450.3\,\mathrm{eV}$, and the plasma can be heated rapidly, as shown by the solid line in Fig. 1(a). The second important thing for the period during the short pulse is to use a pump pulse with a duration so long that it can heat the electron temperature up rapidly while keeping the ion temperature as low as possible. This will be advantageous to enhance the gain coefficient because it is proportional to the electron temperature and inversely proportional to the square root of the ion temperature.

In order to show the hydrodynamic characteristic of the plasma for the short pulse, we investigated the relations of electron temperature, scale length, and electron density with different pulse duration and intensity. The result shows that the electron temperature increases rapidly from 330 eV to 1.84 keV with an increase of pulse duration from 110 fs to 1.1 ps, as shown in Figs. 2(a) and 2(c). At the same time, the scale length increases from 50 to 80 μm with the increase of pulse duration, too, which makes the density gradient more relaxed for the longer pulse than the shorter one, as shown in Fig. 2(b). The electron density is $7.5 \times 10^{20}\,\mathrm{cm^{-3}}$. It is clear that a shorter pulse is not beneficial for the production of an x-ray laser under the same intensity.

For the same pulse duration, the electron temperature increases rapidly from 1.84 to 16.7 keV with an increase of intensity from 5.2×10^{14} to $52 \times 10^{14}\,\mathrm{W/cm^2}$, as shown in Figs. 2(a) and 2(d). This is much more beneficial to enhance the gain coefficient. The scale length increases from 80 to 217 μm, as shown in Fig. 2(b). This is also much more

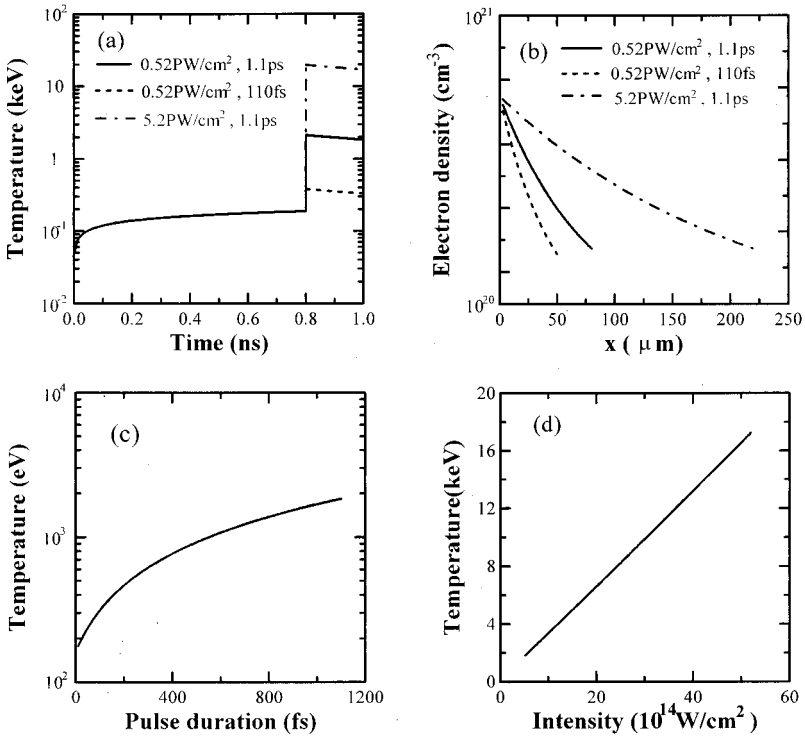

FIG. 2. (a) Temporal history for electron temperature, (b) electron density vs x at the center of the pulse, (c) electron temperature vs the pulse duration while the intensity of the short pulse is being held constant ($5.2\times10^{14}\,\mathrm{W/cm^2}$), and (d) electron temperature vs the intensity while the pulse duration is being held constant (1.1 ps). The conditions are $I_1=0.7\times10^{12}\,\mathrm{W/cm^2}$, $\lambda=1.053\,\mu\mathrm{m}$, $\Delta t_{IL}=0.8\,\mathrm{ns}$, $\Delta t_{2L}=1.1\,\mathrm{ps}$, and $\Delta t_{2L}=110\,\mathrm{fs}$, respectively, with the same intensity $I_2=5.2\times10^{14}\,\mathrm{W/cm^2}$ or $I_2=5.2\times10^{14}\,\mathrm{W/cm^2}$ and $I_2=52\times10^{14}\,\mathrm{W/cm^2}$, respectively, with the same short pulse duration $\Delta t_{2L}=1.1\,\mathrm{ps}$.

beneficial to enhance the total output of x-ray lasers. The results show that the higher the intensity is, the more advantageous it is for the production of the transient population inversion under the same laser duration.

By comparison, we also calculated the case in which there is a delay time between the long and short pulses. The 1-ns delay time is used and other conditions are identical to Dunn's case. The results are shown in Fig. 3. The electron temperature is 110 eV at t_m for the long pulse; it can only ionize Pd to $Z=15.1$, which is not Ni-like ion, as shown by the solid line in Fig. 3(a). But the scale length is increased to 63 μm. This is longer than 40 μm, as shown by the solid line in Fig. 3(b). For the short pulse, the electron temperature is heated rapidly to 2.82 keV. This is higher than 1.84 keV, as shown by the dashed line in Fig. 3(a). The scale length is enhanced to 147 μm. This is about double of 80 μm, as

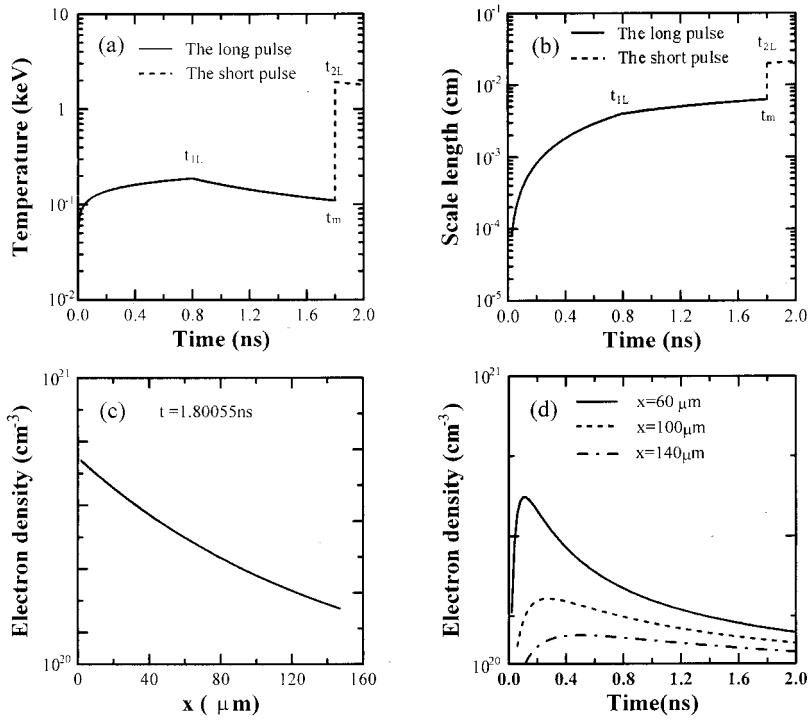

FIG. 3. (a) Temporal history for electron temperature, (b) scaling length history, (c) electron density vs x at the center of the pulse, and (d) electron density history for different x from the similarity equations. The conditions are $I_1=0.7\times10^{12}\,\mathrm{W/cm^2}$, $\lambda=1.053\,\mu\mathrm{m}$, $\Delta t_{IL}=0.8\,\mathrm{ns}$, $I_2=5.2\times10^{14}\,\mathrm{W/cm^2}$, $\Delta t_{2L}=1.1\,\mathrm{ps}$, and the delay time $t_m=1\,\mathrm{ns}$.

shown in Fig. 3(c). The electron density is about $7.1 \times 10^{20}\,\mathrm{cm}^{-3}$. It shows that delay time is not beneficial to enhance the efficiency for the long pulse. However, it can enhance the efficiency for the short pulse, and more importantly it can sufficiently relax the electron density. This can certainly be beneficial for the propagation of an x-ray laser pulse. From this calculation, a conclusion might be possible. An optimum delay time might exist if the propagation of x-ray-laser pulses is considered. This would involve ray-tracing calculation.

V. CONCLUSIONS

In conclusion, we have developed a similarity model for transient x-ray lasers. The calculation results are in agreement with Dunn's experimental results. The results show that a longer long laser pulse can provide higher efficiency, the production of Ni-like ions, and the relaxation of the density gradient, and the high intensity and moderate pulse duration for the short laser pulse are beneficial to enhance both the gain coefficient and scale length. The model is useful for an approximate, quick parameter scan for experimental design and analysis.

ACKNOWLEDGMENTS

This work was supported by the National Nature Science Foundation of China under Grant Nos. 19974074 and 19825110, National High Technology High Power Lasers Program.

[1] J. Zhang *et al.*, Science **276**, 1097 (1997).
[2] F. G. Tomasel, J. J. Rocca, V. N. Shlyaptsev, and C. D. Macchietto, Phys. Rev. A **55**, 1437 (1996).
[3] M. P. Kalachnikov *et al.*, Phys. Rev. A **57**, 4778 (1998).
[4] Y. Li, G. Pretzler, P. Lu, E. E. Fill, and J. Nilson, Phys. Plasmas **4**, 479 (1997).
[5] A. Prag, A. Glinz, J. E. Balmer, Y. Li, and E. Fill, Appl. Phys. B: Lasers Opt. **63**, 113 (1996).
[6] P. V. Nickles *et al.*, Phys. Rev. Lett. **78**, 2748 (1997).
[7] P. J. Warwick *et al.*, J. Opt. Soc. Am. B **15**, 1808 (1998).
[8] J. Dunn *et al.*, Phys. Rev. Lett. **80**, 2825 (1998).
[9] J. Dunn *et al.*, Phys. Rev. Lett. **84**, 4834 (2000).
[10] J. Nilsen, Y. Li, and J. Dunn, J. Opt. Soc. Am. B **17**, 1084 (2000).
[11] J. S. De Groot *et al.*, Phys. Fluids B **4**, 701 (1992).
[12] T. W. Johnston and W. M. Dawson, Phys. Fluids **16**, 722 (1973).
[13] D. Colombant and G. T. Tonon, J. Appl. Phys. **44**, 3524 (1973).
[14] R. A. London and M. D. Rosen, Phys. Fluids **29**, 3813 (1986).